

# The Influence of Sarcoplasmic Reticulum $\text{Ca}^{2+}$ Concentration on $\text{Ca}^{2+}$ Sparks and Spontaneous Transient Outward Currents in Single Smooth Muscle Cells

RONGHUA ZHUGE,\*<sup>†</sup> RICHARD A. TUFT,\*<sup>‡</sup> KEVIN E. FOGARTY,\*<sup>‡</sup> KARL BELLVE,\*<sup>‡</sup> FREDRIC S. FAY,\*<sup>‡†</sup> and JOHN V. WALSH, JR.\*

From the \*Department of Physiology and <sup>‡</sup>Biomedical Imaging Group, University of Massachusetts Medical School, Worcester, Massachusetts 01655

**ABSTRACT** Localized, transient elevations in cytosolic  $\text{Ca}^{2+}$ , known as  $\text{Ca}^{2+}$  sparks, caused by  $\text{Ca}^{2+}$  release from sarcoplasmic reticulum, are thought to trigger the opening of large conductance  $\text{Ca}^{2+}$ -activated potassium channels in the plasma membrane resulting in spontaneous transient outward currents (STOCs) in smooth muscle cells. But the precise relationships between  $\text{Ca}^{2+}$  concentration within the sarcoplasmic reticulum and a  $\text{Ca}^{2+}$  spark and that between a  $\text{Ca}^{2+}$  spark and a STOC are not well defined or fully understood. To address these problems, we have employed two approaches using single patch-clamped smooth muscle cells freshly dissociated from toad stomach: a high speed, wide-field imaging system to simultaneously record  $\text{Ca}^{2+}$  sparks and STOCs, and a method to simultaneously measure free global  $\text{Ca}^{2+}$  concentration in the sarcoplasmic reticulum ( $[\text{Ca}^{2+}]_{\text{SR}}$ ) and in the cytosol ( $[\text{Ca}^{2+}]_{\text{CYTO}}$ ) along with STOCs. At a holding potential of 0 mV, cells displayed  $\text{Ca}^{2+}$  sparks and STOCs.  $\text{Ca}^{2+}$  sparks were associated with STOCs; the onset of the sparks coincided with the upstroke of STOCs, and both had approximately the same decay time. The mean increase in  $[\text{Ca}^{2+}]_{\text{CYTO}}$  at the time and location of the spark peak was  $\sim 100$  nM above a resting concentration of  $\sim 100$  nM. The frequency and amplitude of spontaneous  $\text{Ca}^{2+}$  sparks recorded at  $-80$  mV were unchanged for a period of 10 min after removal of extracellular  $\text{Ca}^{2+}$  (nominally  $\text{Ca}^{2+}$ -free solution with  $50 \mu\text{M}$  EGTA), indicating that  $\text{Ca}^{2+}$  influx is not necessary for  $\text{Ca}^{2+}$  sparks. A brief pulse of caffeine (20 mM) elicited a rapid decrease in  $[\text{Ca}^{2+}]_{\text{SR}}$  in association with a surge in  $[\text{Ca}^{2+}]_{\text{CYTO}}$  and a fusion of STOCs, followed by a fast restoration of  $[\text{Ca}^{2+}]_{\text{CYTO}}$  and a gradual recovery of  $[\text{Ca}^{2+}]_{\text{SR}}$  and STOCs. The return of global  $[\text{Ca}^{2+}]_{\text{CYTO}}$  to rest was an order of magnitude faster than the refilling of the sarcoplasmic reticulum with  $\text{Ca}^{2+}$ . After the global  $[\text{Ca}^{2+}]_{\text{CYTO}}$  was fully restored, recovery of STOC frequency and amplitude were correlated with the level of  $[\text{Ca}^{2+}]_{\text{SR}}$ , even though the time for refilling varied greatly. STOC frequency did not recover substantially until the  $[\text{Ca}^{2+}]_{\text{SR}}$  was restored to 60% or more of resting levels. At  $[\text{Ca}^{2+}]_{\text{SR}}$  levels above 80% of rest, there was a steep relationship between  $[\text{Ca}^{2+}]_{\text{SR}}$  and STOC frequency. In contrast, the relationship between  $[\text{Ca}^{2+}]_{\text{SR}}$  and STOC amplitude was linear. The relationship between  $[\text{Ca}^{2+}]_{\text{SR}}$  and the frequency and amplitude was the same for  $\text{Ca}^{2+}$  sparks as it was for STOCs. The results of this study suggest that the regulation of  $[\text{Ca}^{2+}]_{\text{SR}}$  might provide one mechanism whereby agents could govern  $\text{Ca}^{2+}$  sparks and STOCs. The relationship between  $\text{Ca}^{2+}$  sparks and STOCs also implies a close association between a sarcoplasmic reticulum  $\text{Ca}^{2+}$  release site and the  $\text{Ca}^{2+}$ -activated potassium channels responsible for a STOC.

**KEY WORDS:**  $\text{Ca}^{2+}$  spark • spontaneous transient outward current • Mag-fura-2 •  $[\text{Ca}^{2+}]_{\text{SR}}$  • ryanodine receptor

## INTRODUCTION

$\text{Ca}^{2+}$  signaling has long been treated in terms of global changes in cytosolic  $\text{Ca}^{2+}$  even though  $\text{Ca}^{2+}$  must serve as a signal for many different processes, suggesting that  $\text{Ca}^{2+}$  elevations might be targeted to different regions of the cell or “microdomains.” In recent years, attention has increasingly been drawn to highly localized  $\text{Ca}^{2+}$  changes within the cell. Such highly localized  $\text{Ca}^{2+}$  signals are of importance for two reasons (Ber-

ridge, 1997). First, in many important processes, the global elevation in  $\text{Ca}^{2+}$  is actually the sum of highly localized  $\text{Ca}^{2+}$  elevations due to release from discrete foci in the sarcoplasmic reticulum (SR).<sup>1</sup> Hence, localized elevations can be the “elementary events” underlying a global rise in  $\text{Ca}^{2+}$ . Second, and perhaps even more interestingly, such focal  $\text{Ca}^{2+}$  signals might perform localized and very specific signaling functions in the absence of a global elevation in cytosolic  $\text{Ca}^{2+}$ . For example, localized elevations in  $\text{Ca}^{2+}$  are thought to regulate large conductance  $\text{Ca}^{2+}$ -activated potassium channels

<sup>†</sup>Dr. Fay died on 18 March 1997.

Address correspondence to John V. Walsh, Jr., Department of Physiology, Biomedical Imaging Group, University of Massachusetts Medical Center, Worcester, MA 01605. Fax: 508-856-5997; E-mail: john.walsh@ummed.edu

<sup>1</sup>Abbreviations used in this paper: BK channel,  $\text{Ca}^{2+}$ -activated potassium channel; RyR, ryanodine receptor; SR, sarcoplasmic reticulum; STOC, spontaneous transient outward current.

(BK channels) in the surface membrane of both neurons and smooth muscle cells. Such elevations in  $\text{Ca}^{2+}$  were first postulated by Brown et al. (1983), who called them  $\text{Ca}^{2+}$  "packets" that might serve as "internal transmitters" to explain the spontaneous miniature outward currents caused by activation of groups of BK channels in bullfrog sympathetic ganglion cells.

In cardiac, skeletal, and smooth muscle cells, such transient, localized cytosolic  $\text{Ca}^{2+}$  elevations are called  $\text{Ca}^{2+}$  sparks. In smooth muscle, the existence of  $\text{Ca}^{2+}$  sparks was first inferred from the appearance of spontaneous transient outward currents (STOCs) that are caused by the concerted opening of a number of BK channels and that have been observed in a wide variety of smooth muscle types (Bolton and Imaizumi, 1996). The  $\text{Ca}^{2+}$  sparks that cause STOCs have now been directly observed by others and ourselves in a number of smooth muscle types (Nelson et al., 1995; Kirber et al., 1996; Mironneau et al., 1996; ZhuGe et al., 1998a).

The regulation of  $\text{Ca}^{2+}$  sparks in smooth muscle and other cell types has only recently been addressed. Several regulatory factors for  $\text{Ca}^{2+}$  sparks have been suggested or demonstrated, among them cyclic nucleotides (Porter et al., 1998), cytosolic  $\text{Ca}^{2+}$  (Cheng et al., 1996), and luminal  $\text{Ca}^{2+}$  concentration; that is,  $\text{Ca}^{2+}$  concentration within the sarcoplasmic reticulum ( $[\text{Ca}^{2+}]_{\text{SR}}$ ) (Lukyanenko et al., 1996). In the case of luminal  $\text{Ca}^{2+}$ , possible evidence for its role in regulating sparks comes in a study of ventricular myocytes from phospholamban-deficient knock-out mice (Santana et al., 1997). However, in that study, the level of luminal  $\text{Ca}^{2+}$  was inferred rather than measured directly since there was no way to quantify the actual level of luminal  $\text{Ca}^{2+}$ . Moreover, there is no study of the effects of luminal  $\text{Ca}^{2+}$  on  $\text{Ca}^{2+}$  sparks in smooth muscle and no direct measure of the effect of luminal  $\text{Ca}^{2+}$  on STOCs in any preparation.

It has been postulated that the frequency of STOCs in smooth muscle reflects the level of  $[\text{Ca}^{2+}]_{\text{SR}}$  (Bolton and Imaizumi, 1996), but there has been no direct evidence for this since simultaneous measurements of both STOCs and  $[\text{Ca}^{2+}]_{\text{SR}}$  have not been made. In the present study, we use the low affinity  $\text{Ca}^{2+}$  indicator, mag-fura-2, to make measurements of  $[\text{Ca}^{2+}]_{\text{SR}}$  while monitoring STOCs in a single smooth muscle cell with tight-seal, whole-cell recording. We show that both  $\text{Ca}^{2+}$  sparks and STOCs are abolished upon depletion of SR  $\text{Ca}^{2+}$  and that they recover as the SR reloads. Further, the SR recovers much more slowly than the cytosolic  $\text{Ca}^{2+}$  concentration ( $[\text{Ca}^{2+}]_{\text{CYTO}}$ ). We also demonstrate for the first time by direct measurement a steep relationship between the level of luminal  $\text{Ca}^{2+}$  and the frequency of  $\text{Ca}^{2+}$  sparks and STOCs over a restricted range of  $[\text{Ca}^{2+}]_{\text{SR}}$ . These findings suggest that agents that act to regulate  $\text{Ca}^{2+}$  sparks and STOCs, and hence

the contractile state of smooth muscle, might exert their effects in part by altering  $[\text{Ca}^{2+}]_{\text{SR}}$ .

## METHODS AND MATERIALS

### *Preparation of Cells and Electrophysiology*

Single smooth muscle cells were enzymatically dispersed from the stomach of *Bufo marinus* as described previously (Fay et al., 1982). Membrane currents were recorded with either the Axopatch 1D or Axoclamp 2A (Axon Instruments) in the tight-seal, whole-cell recording configuration. Over 50% of the cells displayed STOCs under the conditions employed. Extracellular solution contained (mM): 130 NaCl, 3 KCl, 1.8  $\text{CaCl}_2$ , 1  $\text{MgCl}_2$ , 10 Hepes, pH adjusted to 7.4 with NaOH. Pipette solution contained (mM): 137 KCl, 3  $\text{MgCl}_2$ , 10 Hepes, 3  $\text{Na}_2\text{ATP}$ , pH adjusted to 7.2 with KOH; free  $[\text{Mg}^{2+}]$  in this solution was calculated to be 0.63 mM. All experiments were carried out at room temperature. Recordings of whole-cell currents were low-pass filtered with the single-pole filter of the Axoclamp 2A (100-Hz cutoff), digitally sampled at 300 Hz, and stored for analysis. In experiments where  $\text{Ca}^{2+}$  sparks were imaged simultaneously with the current, the low frequency cutoff, using the internal four-pole Bessel filter of the Axopatch 1D, was 200 Hz and the sampling rate was 1 kHz. STOCs were detected using a custom algorithm to detect peaks in the current. Peaks were determined using a running average of 18 ms. Once a peak was found, valleys were then checked on either side also using a running average with a window of 18 ms. The valley after the peak was then used as the next starting point to detect the next peak. Net peak current of any found STOC was calculated from the peak current minus the average of the two valley currents. Outward current transients that exceeded 10 pA were counted as STOCs.

### *Measurements of Global $[\text{Ca}^{2+}]$ in Cytosol and SR*

Global  $[\text{Ca}^{2+}]$  was measured using a high temporal resolution microfluorimeter as described previously (Becker et al., 1989). Mag-fura-2 acetoxymethylester (1  $\mu\text{M}$ ) was loaded into the cells as described in RESULTS. For measurements with this dye, fluorescence was converted to  $[\text{Ca}^{2+}]$  (Grynkiewicz et al., 1985) using a  $K_d$  for  $\text{Ca}^{2+}$ -mag-fura-2 of 54  $\mu\text{M}$ ; determining  $R_{\text{max}}$ ,  $R_{\text{min}}$ , and  $\beta$  as previously described (Becker and Fay, 1987). In the absence of  $\text{Mg}^{2+}$ , this calculation gave a resting mean  $[\text{Ca}^{2+}]_{\text{SR}}$  of 154  $\mu\text{M}$  determined in 172 cells. This calibration depends on a variety of factors, which cannot be determined with certainty in vivo (Golovina and Blaustein, 1997). However, in A7r5 cells, a cell line derived from smooth muscle, Sugiyama and Goldman (1995) found that alterations in  $[\text{Mg}^{2+}]_{\text{SR}}$ , ranging from 0 to 20 mM, did not alter the mag-fura-2 fluorescence ratio when  $[\text{Ca}^{2+}]_{\text{SR}}$  was held constant at 100  $\mu\text{M}$ . From these and other observations, Sugiyama and Goldman (1995) concluded that, with the diminished  $\text{Mg}^{2+}$  sensitivity of mag-fura-2 in the presence of the relatively high  $[\text{Ca}^{2+}]$  of the SR, measurements of changes in  $[\text{Ca}^{2+}]_{\text{SR}}$  were unlikely to be changed significantly by concomitant changes in  $[\text{Mg}^{2+}]_{\text{SR}}$  (see also Hofer and Schulz, 1996; Quamme et al., 1993). Finally, our conclusions here depend on changes in  $[\text{Ca}^{2+}]_{\text{SR}}$ , not on absolute values. In those experiments where global  $[\text{Ca}^{2+}]_{\text{SR}}$  and  $[\text{Ca}^{2+}]_{\text{CYTO}}$  were measured simultaneously in the same cell, we used a custom-built, high-speed multiple-wavelength microfluorimeter equipped with a 150-W xenon lamp. In such experiments,  $\text{Ca}^{2+}$  Green-1 dextran, potassium salt (mol wt 3000, 10  $\mu\text{M}$ ) was introduced via the patch pipette into cells preloaded with mag-fura-2 acetoxymethylester (see RESULTS) and excited at 490 nm. Mag-fura-2 was excited at 340 and 380 nm. Every 20 ms, the fluorescence was mea-

sured at 535 nm for a period of 5 ms for each excitation wavelength. For  $\text{Ca}^{2+}$  Green measurements,  $[\text{Ca}^{2+}]_{\text{CYTO}}$  was calculated as described previously (Hernandez-Cruz et al., 1990), taking the resting  $[\text{Ca}^{2+}]_{\text{CYTO}}$  as 100 nM based on previous measurements in these cells using fura-2 (Drummond and Fay, 1996).

### Digital Imaging of $\text{Ca}^{2+}$ Sparks

Fluorescence images of cytosolic free  $\text{Ca}^{2+}$  using fluo-3 as a calcium indicator were achieved using a custom-built wide-field digital imaging system or ultrafast microscope (see Fig. 1). The system can acquire images at a maximum speed of 543 Hz, thus providing a temporal resolution comparable to the confocal line-scan technique, but with a much larger observed area. Such rapid imaging was made possible by equipping the system with a cooled high-sensitivity, charge-coupled device camera developed in conjunction with the Massachusetts Institute of Technology Lincoln Laboratory (Lexington, MA; see Fig. 1, legend). The camera was interfaced to a custom made inverted microscope. The 488 nm line of an Argon Ion laser (Coherent) provided fluorescence excitation, and a laser shutter controlled the exposure duration. Emission of the  $\text{Ca}^{2+}$  indicator was monitored at wavelengths  $>500$  nm. Subsequent image processing and analysis was performed off line using a custom-designed software package, running on a Silicon Graphics workstation.  $\text{Ca}^{2+}$  images were derived on a pixel to pixel basis from the equation  $\Delta F/F_0 (\%) = 100 \times [F(x,y,t) - F_0(x,y)]/F_0(x,y)$ , where  $F(x,y,t)$  is the fluorescence at each pixel in the time series and  $F_0$  is an image of the "resting" level given by the average of several images over time in the

absence of sparks. The change in fluorescence provides only a relative, not an absolute, measurement of free  $\text{Ca}^{2+}$  concentration. An increase in fluorescence was considered to be a  $\text{Ca}^{2+}$  spark when it was  $\geq 5.0\%$  and lasted for at least two 10-ms frames. The root mean square (rms) noise, following smoothing of the images with a three-by-three pixel approximation to a Gaussian, was both measured from the data and calculated from the noise properties of the CCD camera; it was 1.5% in each case. Thus, the threshold for a spark, 5%, was more than three times greater than the rms noise.

### Data Analysis and Reagents

Data are reported as mean  $\pm$  SEM, and  $n$  refers to the number of cells. Statistical analysis of difference was made with paired or unpaired Student's  $t$  test, as appropriate, with  $P < 0.05$  considered significant. Mag-fura-2, fluo-3, and  $\text{Ca}^{2+}$  Green-1 were purchased from Molecular Probes, Inc., and all other chemicals from Sigma Chemical Co.

## RESULTS

### $\text{Ca}^{2+}$ Sparks and STOCs Recorded in the Same Cell

To establish the relationship between  $\text{Ca}^{2+}$  sparks and STOCs, we first recorded both events simultaneously in the same cell using the ultrafast microscope diagrammed in Fig. 1 and standard patch clamp method-

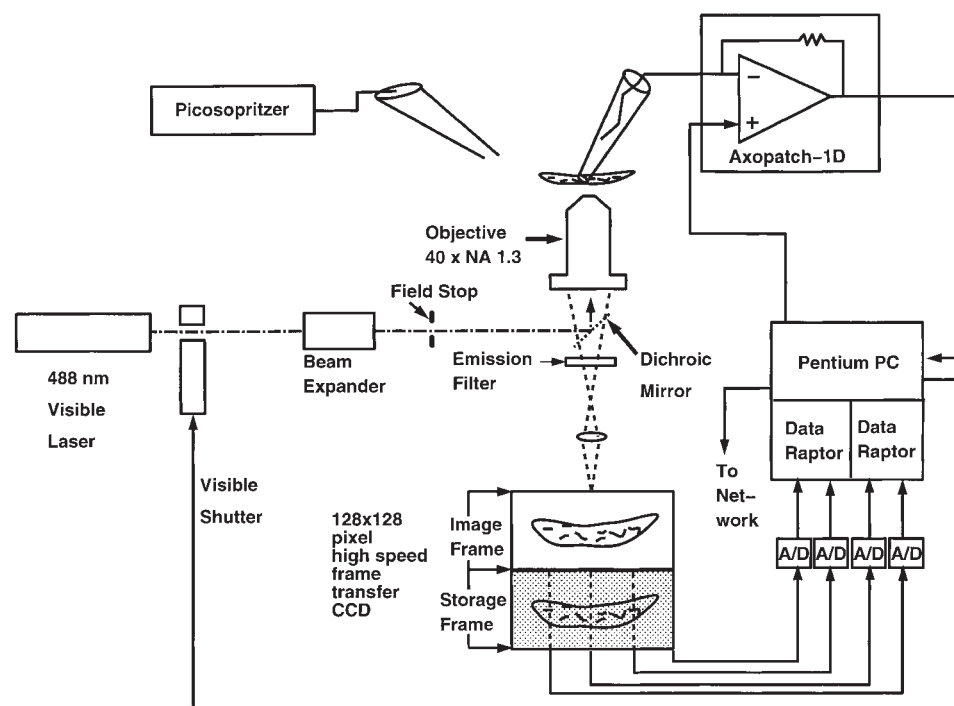


FIGURE 1. Schematic illustration of the ultrafast digital imaging system used to collect two-dimensional images of fluo-3 fluorescence. The beam of an Argon laser, tuned to  $\lambda = 488$  nm, is passed through an electronically controlled shutter and telescopic beam expander. A field stop iris diaphragm typically limits the illumination to a region of the specimen  $\sim 100 \mu\text{m}$  in diameter. The expanded beam is reflected by a dichroic mirror in the body of a custom-built epifluorescence microscope, passes through the objective ( $40\times 1.3$  NA Nikon oil immersion) and illuminates the cell. The fluo-3 fluorescence is collected by the objective, passes through the dichroic mirror and a 500-nm long-pass emission filter, and is imaged onto a high-speed, low-noise (70% quantum efficiency, 6.5 electrons root mean square readout noise), thermoelectrically cooled frame transfer CCD camera. The camera im-

age frame is an array of  $128 \times 128$   $24\text{-}\mu\text{m}$  square pixels; the storage frame is of identical size. The detected image is shifted from the image to the storage frame in  $50 \mu\text{s}$ , and the storage frame read out in 1.8 ms. Since acquisition of a new image can begin as soon as the image frame is cleared, the maximum camera rate is 543 frames/s. In this experiment, images were integrated for 10 ms and read out immediately, resulting in an image rate of 100 images/s. Each pixel samples a  $333\text{-nm}$  square of the specimen. The camera has four digital outputs connected to two frame grabber boards (Data Raptor; Bitflow Inc.) connected to the PCI bus of a Pentium 90 MHz PC. The images are collected and stored in frame grabber memory, which can hold 8 MB of information, and later transferred to disk archival storage. The PC has an analogue to digital converter that digitizes the whole cell patch clamp current as well as the position of the objective, the image readout times, and membrane potential. Thus, the exact timing of the electrophysiological events in relation to the acquired images is known. Patch clamp recordings are done with an Axopatch 1D patch clamp amplifier. Agents are applied by pressure ejection with a Picospritzer II (General Valve Corp.).

ology (Hamill et al., 1981). The  $\text{Ca}^{2+}$  indicator fluo-3 (50  $\mu\text{M}$ ) was loaded into the cells through the patch pipette. At a holding membrane potential of 0 mV, the smooth muscle cells displayed  $\text{Ca}^{2+}$  sparks and coincident STOCs as illustrated in Fig. 2. Each spark was associated with a STOC in this sequence, with both spark and STOC rising simultaneously. (However, the spark for each STOC is not evident since whole-cell patch recording registers all STOCs in the cell, whereas the image captures only a portion of the cell.) In this smooth muscle cell type, the mean half time of spark decay ( $\sim 20$  ms) was close to that of the STOCs ( $17.0 \pm 1.7$  ms;  $n = 15$  cells). The mean amplitudes of  $\text{Ca}^{2+}$  sparks

and STOCs were  $10.8 \pm 0.2\%$  and  $27.2 \pm 5.2$  pA ( $n = 15$  cells), respectively.

The  $\text{Ca}^{2+}$  sparks were visible as distinct, isolated events restricted to a small area of the cell, usually covering  $< 3 \mu\text{m}^2$  at the time of their peak amplitude. Hence, they are quite different from the  $\text{Ca}^{2+}$  waves seen in many cell types. For a given cell, there were multiple spark-generating foci, with each focus discharging in an apparently random way. Moreover, it appeared that some foci discharged at a much higher rate than others and thus may constitute "hot spots," similar to those first identified in esophageal smooth muscle cells (Kirber et al., 1998; see also Gordienko et al.,

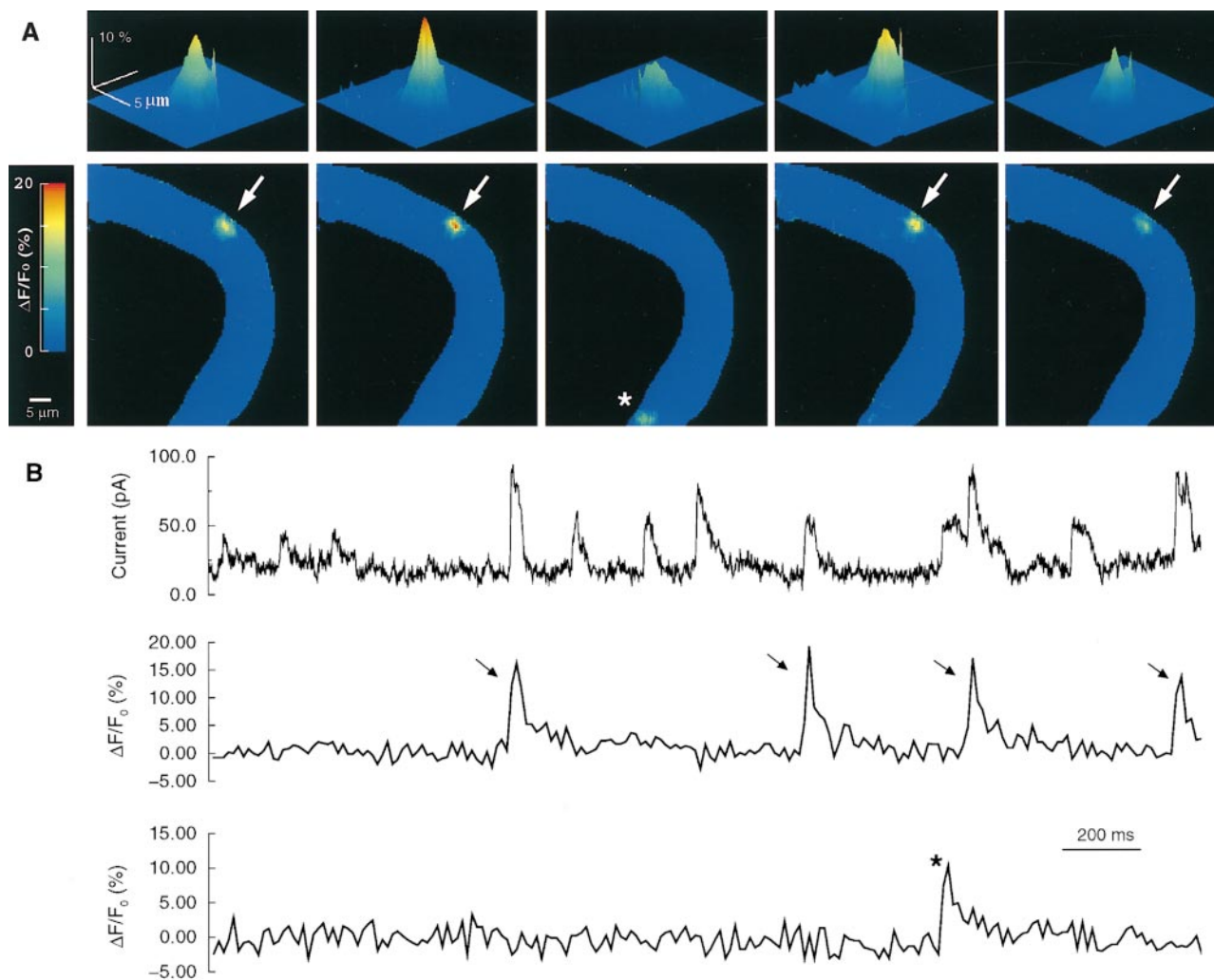


FIGURE 2.  $\text{Ca}^{2+}$  sparks and STOCs recorded simultaneously in a single smooth muscle cell.  $\text{Ca}^{2+}$  sparks were monitored with the ultrafast microscope while membrane currents were recorded in the tight-seal, whole-cell mode as described in METHODS. The patch pipette contained 50  $\mu\text{M}$   $\text{K}_5$  fluo-3. Approximately 10 min after rupturing the patch membrane, two-dimensional fluorescence images were acquired continuously at a rate of 100 Hz. After low-pass filtering at 200 Hz, the membrane current was digitally sampled at 1 kHz at a holding potential of 0 mV. (A) Images (10-ms exposures) of fluo-3 fluorescence showing five  $\text{Ca}^{2+}$  sparks from two sites, four at one site (arrows) and one at the other (\*), during a 2-s recording period. These images were obtained at the time of the peak spark intensity (B, middle and bottom). The images in A, top, show the  $\text{Ca}^{2+}$  sparks below with a surface plot at higher spatial magnification. (B, top) Continuous records of whole-cell currents. (Middle and bottom) Continuous records of fluorescence intensity for two different pixels, each  $333 \times 333$  nm. (Middle) Fluorescence for the pixel at the center of the sparks indicated by the arrows; (bottom) fluorescence for the pixel at the center of the spark indicated by the asterisk.

1998). For example, in Fig. 2, there were two spark-generating foci in the approximately one third of the cell surveyed in this case during the 2-s time period shown. Whereas one focus discharged only once, the other discharged four times.

The coincidence and similar time course of  $\text{Ca}^{2+}$  sparks and STOCs provide strong evidence that sparks are responsible for generating STOCs. To further examine this point, we tested the effect of altering spark frequency on STOC generation. To do so, we employed caffeine, which is known to cause  $\text{Ca}^{2+}$  release from internal stores through activation of ryanodine receptors (RyRs), which presumably underlie  $\text{Ca}^{2+}$  sparks in smooth muscle, as is the case in other preparations (Cheng et al., 1993; Xu et al., 1994; Nelson et al., 1995; Tsugorka et al., 1995). In the presence of 0.5 mM caffeine at a holding potential of 0 mV, a lower concentration than was used to deplete the SR and abolish sparks and STOCs in these cells (see below), there was an increase in frequency of both sparks (a 2.2-fold increase from  $1.3 \pm 0.4/\text{s}$  to  $2.9 \pm 0.4/\text{s}$ ; 184 sparks in five cells;  $P < 0.05$ ) and STOCs (a 2.4-fold increase from  $2.5 \pm 0.7/\text{s}$  to  $5.9 \pm 1.1/\text{s}$ ; 443 STOCs in the same five cells;  $P < 0.05$ ). Hence, consistent with earlier studies on other smooth muscle cells (Nelson et al., 1995; Mironneau et al., 1996), STOCs in these cells are due to  $\text{Ca}^{2+}$  sparks. That STOCs are caused by sparks does not im-

ply, however, that every spark causes a STOC; in some instances we observed sparks that failed to cause STOCs (see also Kirber et al., 1998).

#### STOCs are Due to BK Channels

In other types of smooth muscle, STOCs are thought to result from coincident openings of a cluster of BK channels (Bolton and Imaizumi, 1996). To establish the identity of channels underlying the STOCs in these cells, we examined the effects of extracellular  $\text{K}^+$  and iberiotoxin, a specific inhibitor of BK channels (Galvez et al., 1990). In normal (3 mM) extracellular  $\text{K}^+$ , STOC activity was apparent at holding potentials of  $-60$  mV or more positive, with greater amplitude at more positive potentials (Fig. 3 A, top), consistent with the voltage dependence of STOCs in other smooth muscle preparations (Bolton and Imaizumi, 1996). In 45 mM extracellular  $\text{K}^+$  (Fig. 3 A, middle), the STOCs reversed in sign in the region of  $-20$  mV, close to the calculated  $\text{K}^+$  reversal potential of  $-25$  mV for these cells. Moreover, the STOCs induced by depolarization were eliminated by 100 nM iberiotoxin (Fig. 3 B), as expected for events caused by BK channels. Finally, it is of considerable interest that STOCs occur at a potential of  $-80$  mV (Fig. 3 A, bottom), given the  $\text{Ca}^{2+}$  sensitivity of BK channels in these cells (see DISCUSSION).

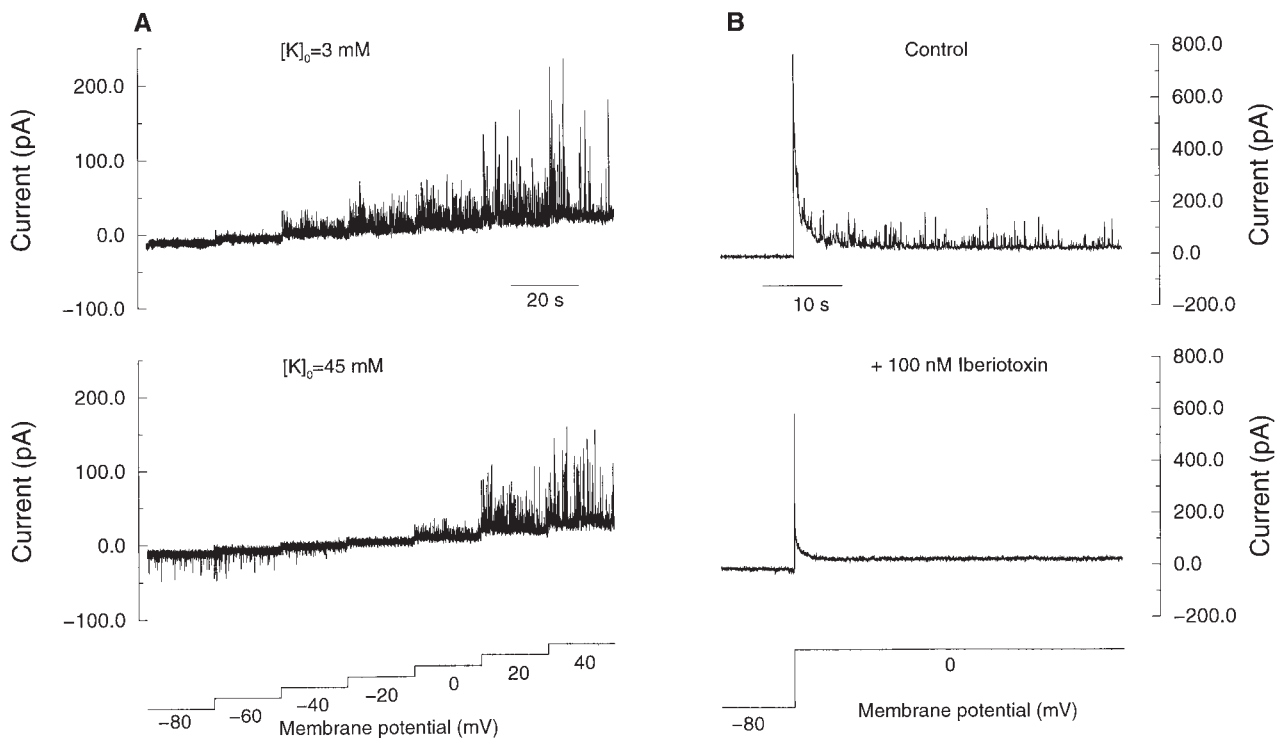


FIGURE 3. STOCs arise from openings of BK channels. (A) Dependence of STOCs on extracellular  $\text{K}^+$  and membrane potential. The voltage was increased in stepwise fashion, as shown, at two different concentrations of external  $\text{K}^+$ . (B) Blockade of STOCs by iberiotoxin (100 nM).

### *Ca<sup>2+</sup> Sparks Occur in the Absence of Extracellular Ca<sup>2+</sup>*

Considerable evidence has accumulated in other smooth muscle cells and in neurons that the Ca<sup>2+</sup> causing STOCs is from an intracellular source as opposed to entry through the surface membrane (Brown et al., 1983; Bolton and Imaizumi, 1996). This is consistent with the idea that STOCs are caused by Ca<sup>2+</sup> sparks and that Ca<sup>2+</sup> sparks are due to release of Ca<sup>2+</sup> from intracellular stores. To establish the source of Ca<sup>2+</sup> sparks in these cells, we tested whether spontaneous Ca<sup>2+</sup> sparks that occur at -80 mV are independent of extracellular Ca<sup>2+</sup>. As shown in Fig. 4, the frequency and amplitude of the sparks were unchanged in the presence and absence of extracellular Ca<sup>2+</sup> at this holding potential. (To eliminate extracellular Ca<sup>2+</sup>, 50  $\mu$ M EGTA was added to a nominally Ca<sup>2+</sup>-free solution. Sparks were then monitored for a period that ranged from 3 to 10 min after superfusion with this solution. Longer periods in Ca<sup>2+</sup>-free solution were not employed to avoid effects due to possible depletion of intracellular stores.) Spark amplitude and rate were  $10.9 \pm 0.93\%$  and  $0.5 \pm 0.24/s$ , respectively, in the presence of extracellular Ca<sup>2+</sup>, values that were not significantly different from  $9.4 \pm 0.9\%$  and  $0.45 \pm 0.30/s$  in its absence ( $n = 4$  cells). Hence, Ca<sup>2+</sup> sparks do not require Ca<sup>2+</sup> entry through the surface membrane. We then went on to establish in direct fashion that SR Ca<sup>2+</sup> is the source of Ca<sup>2+</sup> sparks and therefore the cause of STOCs.

### *Mag-Fura-2 Measures [Ca<sup>2+</sup>]<sub>SR</sub>*

To directly evaluate the role of [Ca<sup>2+</sup>]<sub>SR</sub> in the generation of Ca<sup>2+</sup> sparks and STOCs, we employed the following method to measure Ca<sup>2+</sup> in internal stores based on techniques used in other cell types (Hofer and Machen, 1993; Chatton et al., 1995; Mlinar and Fay, 1995). Cells were incubated with the esterified form of the low affinity calcium indicator, mag-fura-2. Upon entering the cells, mag-fura-2 acetoxymethylester was hydrolyzed and trapped both in the cytosol and other intracellular compartments (Williams et al., 1985). A tight-seal, whole-cell patch recording configuration was then used to dialyze the cytosol against the contents of the patch pipette. Upon rupture of the patch membrane, the fluorescence ratio gradually increased (Fig. 5 A), indicating that the nondialyzable dye was trapped in a compartment containing higher free [Ca<sup>2+</sup>] than that in the bulk cytosol. The following experiments were carried out to determine if this compartment was indeed the SR.

Since caffeine activates RyRs causing Ca<sup>2+</sup> release from the SR (Xu et al., 1994), the effect of caffeine on the mag-fura-2 signal was examined. As shown in Fig. 5 B, the fluorescence ratio decreased rapidly in response to caffeine (20 mM). After cessation of caffeine applica-

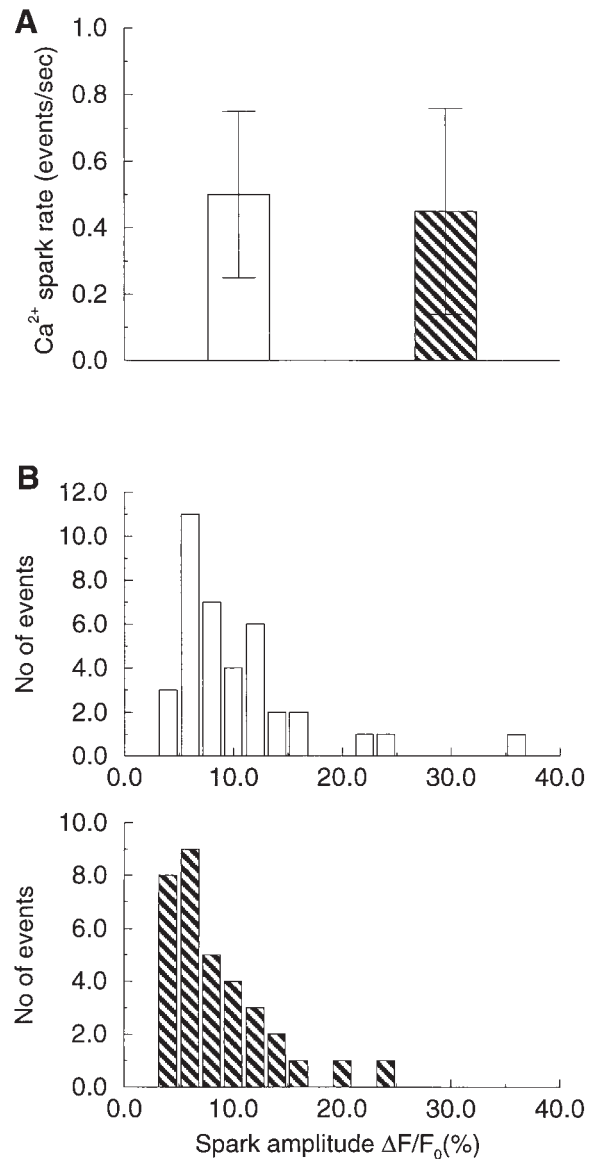
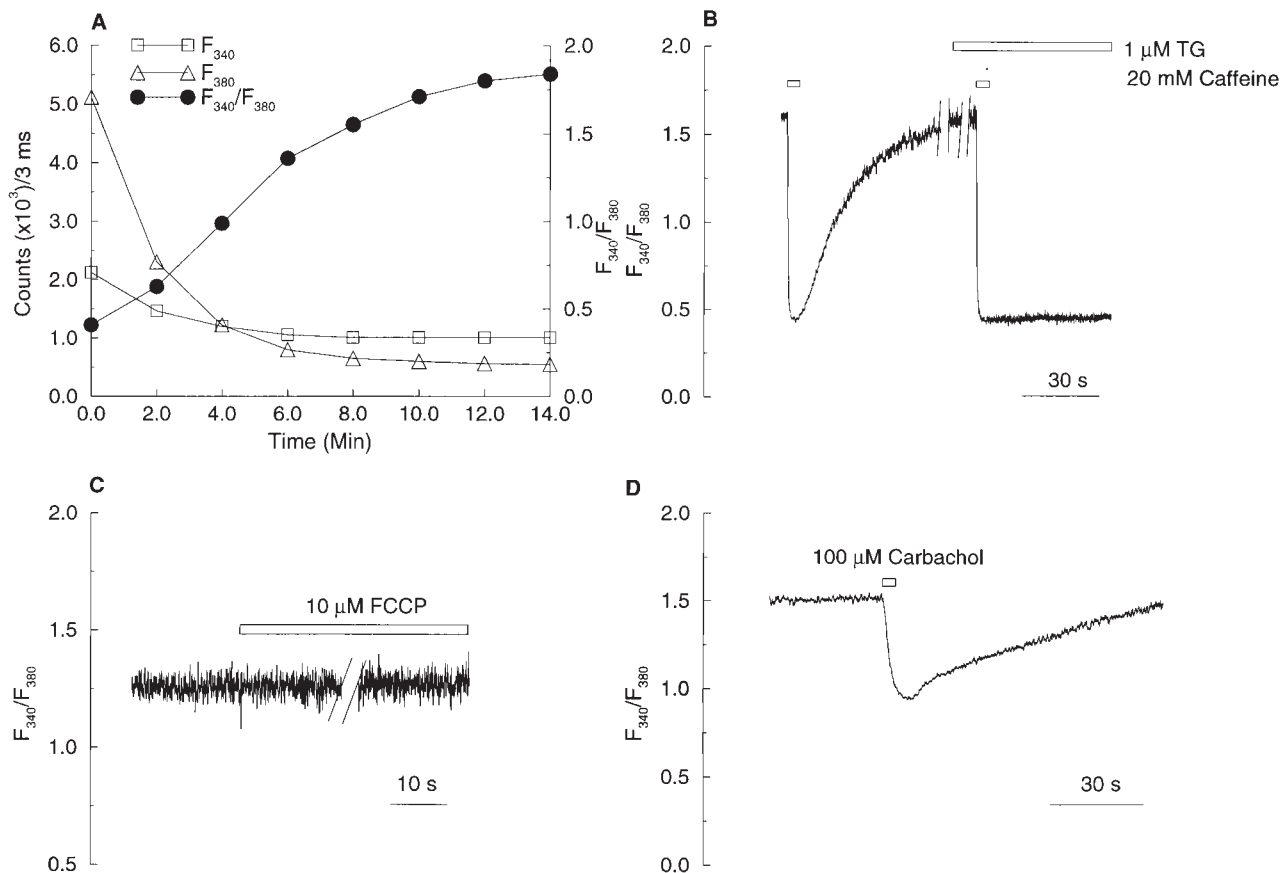


FIGURE 4. Ca<sup>2+</sup> sparks occur without Ca<sup>2+</sup> entry through the surface membrane. At a holding potential of -80 mV, Ca<sup>2+</sup> sparks were recorded from each cell in the presence of extracellular Ca<sup>2+</sup> (1.8 mM), and then for a period of 10 min or less after removal of extracellular Ca<sup>2+</sup>. The Ca<sup>2+</sup>-free environment was established by superfusing cells with nominally Ca<sup>2+</sup>-free solution containing 50  $\mu$ M EGTA. The spark rate (A) and amplitude (B) were the same in the presence (open bars) and absence (striped bars) of extracellular Ca<sup>2+</sup>.

tion, the fluorescence ratio recovered back towards its prestimulus level, but this recovery was completely blocked in the presence of 1  $\mu$ M thapsigargin (Fig. 5 B), an inhibitor of SR calcium pumps (Thastrup et al., 1990). In contrast, a mitochondrial uncoupler, the protonophore carbonyl cyanide *p*-trifluoromethoxy-phenylhydrazone (1  $\mu$ M), which inhibits Ca<sup>2+</sup> uptake by mitochondria in these cells (Drummond and Fay, 1996), had no effect on the mag-fura-2 fluorescence ratio (Fig.



**FIGURE 5.** Mag-fura-2 detects free  $\text{Ca}^{2+}$  concentration in sarcoplasmic reticulum. (A) After loading of mag-fura-2 into the cytoplasm and the intracellular stores by incubation with the esterified form of the dye, tight-seal whole-cell recording was begun at time 0, which denotes the occurrence of membrane breakthrough. Fluorescence from a no-nuclear region of the cell was sampled for 10 s at 2-min intervals as shown. The fluorescence ratio increased as dye was dialyzed away, indicating that the dye remaining in the cell was trapped in a compartment with high  $[\text{Ca}^{2+}]$ . (B) Mag-fura-2 signal in single smooth muscle cells responds to caffeine and thapsigargin (TG), consistent with localization of the dye in the SR. Trace shows effect of caffeine before and after treatment with TG on the fluorescence ratio in a single cell dialyzed as in A. The recording was stopped for 5 min (first gap) after the first brief application of caffeine; it was stopped again for 5 min after application of 1  $\mu\text{M}$  TG (second gap). Note that by itself TG had no effect on fluorescence ratio over this 5-min period, as is evident by the fact that the trace did not shift after the second 5-min gap. Caffeine (20 mM) was applied locally from a puffer pipette for 3 s at the times indicated by the bars. (C) Mag-fura-2 signal did not change in response to the application of the mitochondria uncoupler carbonyl cyanide *p*-trifluoromethoxy-phenylhydrazone (FCCP; 1  $\mu\text{M}$ ). The recording was stopped for 3 min as indicated by the gap in the trace. (D) Carbachol (100  $\mu\text{M}$ ) applied locally for 3 s induced a decrease in the mag-fura-2 ratio, consistent with an SR localization of the indicator.

5 C). Carbachol (100  $\mu\text{M}$ ), an inositol 1,4,5-trisphosphate-producing agent, caused a decrease followed by a recovery in fluorescence ratio, although this decrease was less than that caused by 20 mM caffeine (Fig. 5 D). In another set of experiments, inclusion of 100  $\mu\text{M}$  ryanodine (Xu et al., 1994) in the patch pipette also led to a decline in the mag-fura-2 fluorescence ratio, albeit more slowly, to about the same level observed with caffeine (data not shown). In summary, the sensitivity of the mag-fura-2 signal to agents known to act on the SR indicates that the mag-fura-2 signal arises principally from the SR in these cells. This conclusion is also supported by an earlier demonstration that mag-fura-2 displays the same submembranous distribution pattern in these cells as does calsequestrin, which is localized to

SR (Steenbergen and Fay, 1996). Finally, mag-fura-2 has also been demonstrated to be a reliable indicator of  $[\text{Ca}^{2+}]_{\text{SR}}$  in A7r5 cells, a cell line derived from rat aorta smooth muscle cells (Sugiyama and Goldman, 1995).

*The Relationship between  $[\text{Ca}^{2+}]_{\text{SR}}$  and STOCs: Simultaneous Measurements of  $[\text{Ca}^{2+}]_{\text{CYTO}}$ ,  $[\text{Ca}^{2+}]_{\text{SR}}$ , and STOCs*

Having established the methods to directly measure  $[\text{Ca}^{2+}]_{\text{SR}}$ , we then sought to examine the relationship between  $[\text{Ca}^{2+}]_{\text{SR}}$ ,  $[\text{Ca}^{2+}]_{\text{CYTO}}$ , and the generation of STOCs. To do so, we simultaneously monitored, at high temporal resolution, mag-fura-2 fluorescence originating from the SR and  $\text{Ca}^{2+}$  Green fluorescence

originating from the cytosol. We used the same experimental approach as above to load mag-fura-2, but for these experiments  $\text{Ca}^{2+}$  green was included in the patch pipette. Brief exposure to caffeine (Fig. 6) caused a prompt release of  $\text{Ca}^{2+}$  from the SR, as indicated by a rise in  $[\text{Ca}^{2+}]_{\text{CYTO}}$  and a fall in  $[\text{Ca}^{2+}]_{\text{SR}}$ .  $[\text{Ca}^{2+}]_{\text{CYTO}}$  returned rapidly ( $t_{1/2} = 4.6 \pm 0.7$  s) to normal resting levels, whereas it took well over  $10\times$  as long for the  $[\text{Ca}^{2+}]_{\text{SR}}$  to return to its resting level ( $t_{1/2} = 62.8 \pm 5.8$  s;  $n = 12$ ). As can be seen from Fig. 6, the recovery of the STOCs began well after global  $[\text{Ca}^{2+}]_{\text{CYTO}}$  had returned to an unchanging resting level and hence STOC frequency is not a function of global  $[\text{Ca}^{2+}]_{\text{CYTO}}$  during this period.

We next analyzed STOC activity during the period after  $[\text{Ca}^{2+}]_{\text{CYTO}}$  had returned to rest and while the SR was still refilling. Although the refilling of the SR was always at least an order of magnitude slower than the restoration of  $[\text{Ca}^{2+}]_{\text{CYTO}}$  to resting levels after caffeine application (see DISCUSSION), there was considerable variation from cell to cell in the rate of SR refilling. Based on the rate of restoration of  $[\text{Ca}^{2+}]_{\text{SR}}$ , we grouped the cells into two classes: "fast" ( $[\text{Ca}^{2+}]_{\text{SR}}$  re-

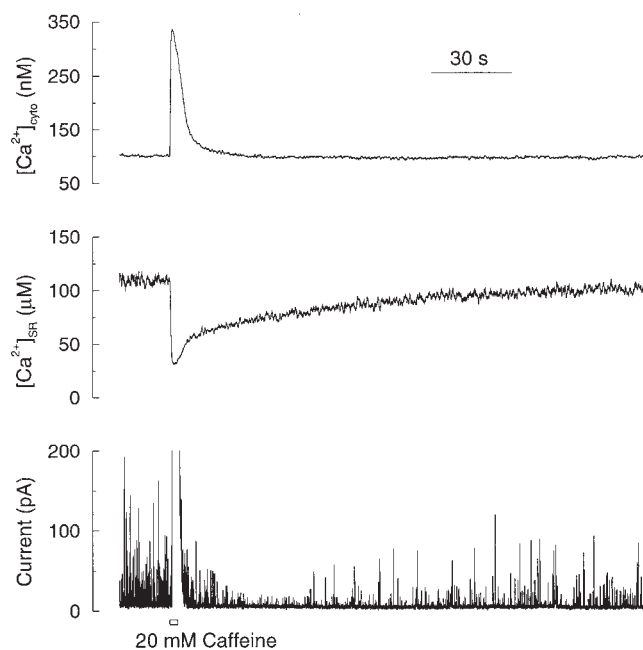


FIGURE 6. The reappearance of STOCs after a brief caffeine stimulation is correlated with refilling of SR with  $\text{Ca}^{2+}$ , but not with global  $[\text{Ca}^{2+}]_{\text{CYTO}}$ .  $[\text{Ca}^{2+}]_{\text{CYTO}}$  (top),  $[\text{Ca}^{2+}]_{\text{SR}}$  (middle), and STOCs (bottom) at rest and in response to a brief (3-s) caffeine application measured simultaneously in a single smooth muscle cell voltage clamped at 0 mV.  $[\text{Ca}^{2+}]_{\text{SR}}$  was determined ratiometrically using mag-fura-2 as outlined above.  $[\text{Ca}^{2+}]_{\text{CYTO}}$  was determined from changes in the fluorescence of  $\text{Ca}^{2+}$  Green using a value for resting  $[\text{Ca}^{2+}]_{\text{CYTO}}$  of 100 nM. (The current record is briefly interrupted shortly after caffeine application as the recording saturated at the gain required to observe STOCs for the majority of the recording.)

stored to the precaffeine level in 200 s or less) and "slow" (full SR recovery not achieved within 200 s). The mean time for recovery to 80% of precaffeine levels for the fast and slow groups was  $47.8 \pm 18.0$  s ( $n = 4$ ) and  $174.9 \pm 17.3$  s ( $n = 5$ ), respectively. Representative examples of recovery from a cell in the fast and slow groups are shown in Fig. 7 A. Once STOCs ceased following discharge of  $\text{Ca}^{2+}$  from the SR, they reappeared at appreciable frequency only after the SR refilled to 60% or more of the resting level. The recovery of STOC frequency and amplitude after caffeine application is plotted as a function of normalized  $[\text{Ca}^{2+}]_{\text{SR}}$  in Fig. 7 B. Despite the substantial variation in recovery time, both the fast and slow groups show the same relationship between  $[\text{Ca}^{2+}]_{\text{SR}}$  and STOCs, indicating that the lapse of time after caffeine application did not account for the change in STOC function. STOC frequency generally showed the most marked recovery at levels in excess of 80% of resting  $[\text{Ca}^{2+}]_{\text{SR}}$  (Fig. 7 B). Thereupon, STOC frequency increased steeply with progressive refilling of the SR so that the relationship between  $[\text{Ca}^{2+}]_{\text{SR}}$  and STOC frequency was most marked as the original precaffeine level was approached. Not only did the frequency of STOCs increase with refilling, but their amplitude also increased as expected on the basis of an increase in the electrochemical gradient for  $\text{Ca}^{2+}$  across the SR membrane. However, the increase in STOC amplitude was more linear than the increase in frequency.

#### Relationship between $[\text{Ca}^{2+}]_{\text{SR}}$ and $\text{Ca}^{2+}$ Sparks

The dependence of STOCs on the degree of SR  $\text{Ca}^{2+}$  refilling suggests that  $\text{Ca}^{2+}$  sparks should also show the same dependence. However, since BK channel activity can be affected by factors other than  $\text{Ca}^{2+}$  sparks, it is possible that the  $\text{Ca}^{2+}$  sparks might bear a different relationship to  $[\text{Ca}^{2+}]_{\text{SR}}$ . Hence, we also examined the time course of  $\text{Ca}^{2+}$  spark recovery after SR depletion with caffeine. After a 3-s caffeine application,  $\text{Ca}^{2+}$  sparks were imaged for a 2-s period at intervals of 30 s. The results of these experiments are given in Fig. 8 A, where spark frequency ( $\bullet$ ) and amplitude ( $\square$ ) are plotted as a function of the time after caffeine application. Software limitations of the digital imaging system presently preclude simultaneous measurements of  $\text{Ca}^{2+}$  sparks at high time resolution and  $[\text{Ca}^{2+}]_{\text{SR}}$ . However, the relationship between the time course of refilling and the level of  $[\text{Ca}^{2+}]_{\text{SR}}$  at each point in time allowed us to determine the approximate relationship between  $[\text{Ca}^{2+}]_{\text{SR}}$  and  $\text{Ca}^{2+}$  spark recovery. (The recovery of the STOC frequency and amplitude within 200 s in these cells indicated that SR refilling was essentially complete within this time and hence followed a fast time course; see Fig. 7 A.) The pattern of recovery of the  $\text{Ca}^{2+}$  sparks was qualitatively similar to that of the

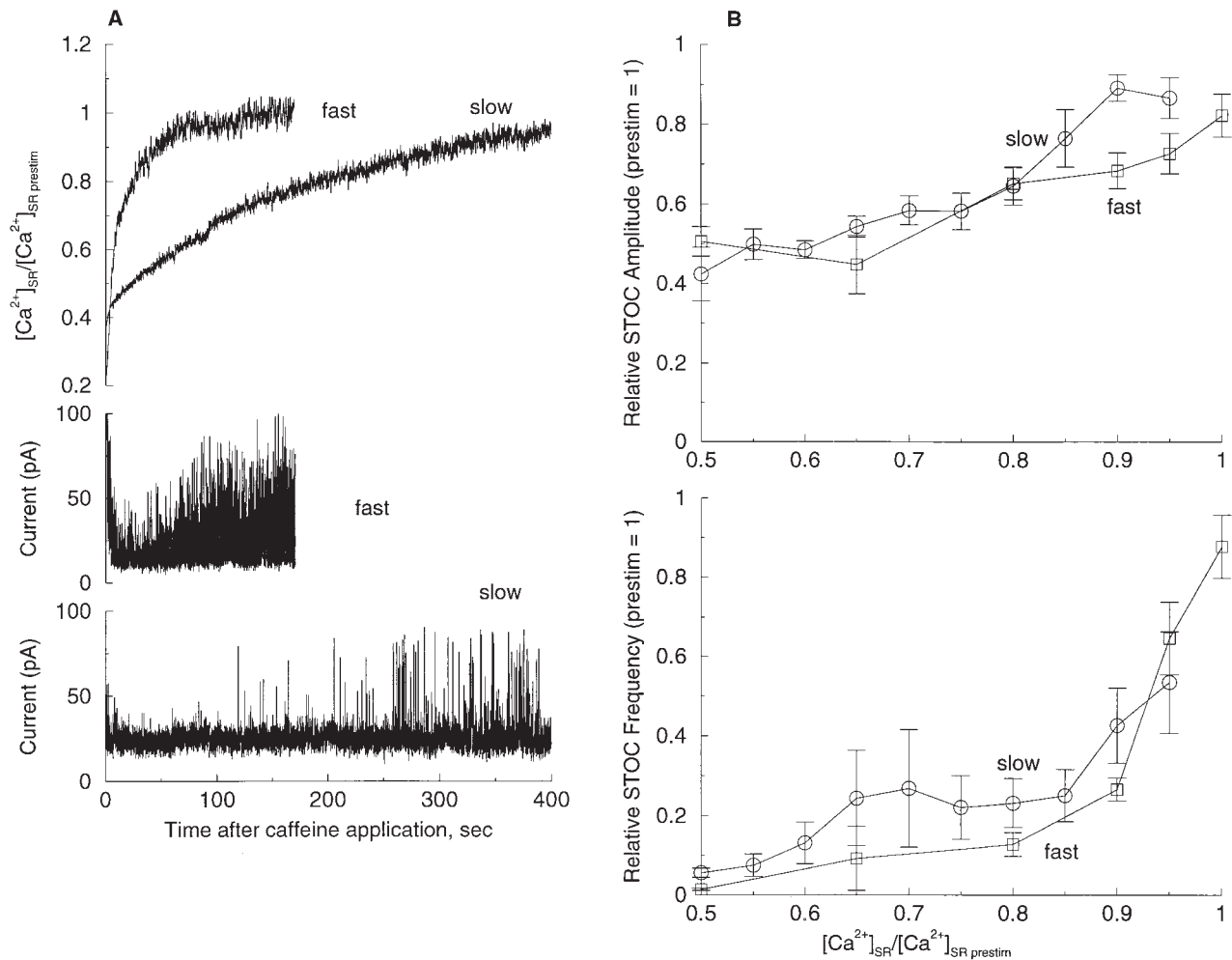


FIGURE 7. STOC frequency and amplitude are functions of luminal  $[Ca^{2+}]_{SR}$  regardless of refilling rate. (A) Recordings from representative cells showing fast and slow recovery of  $[Ca^{2+}]_{SR}$  and corresponding STOCs. Time course of normalized  $[Ca^{2+}]_{SR}$  for the two cells (top) and STOCs (middle and bottom) after 3-s caffeine application that ended at time 0. (B) STOC amplitude (top) and frequency (bottom) as a function of  $[Ca^{2+}]_{SR}$  as the SR reloads after a 3-s caffeine application. STOC frequency and amplitude were determined for intervals in each record corresponding to 5% increases (for slowly refilling cells) and 10 or 15% increases (for fast refilling cells) in  $[Ca^{2+}]_{SR}$  during refilling. The data for each of the cells (four in the fast group and five in the slow group) are normalized to the values in each cell before caffeine application.

STOCs (Fig. 8 B). That is, there was a steep relation between  $Ca^{2+}$  spark frequency and  $[Ca^{2+}]_{SR}$  at levels when the  $[Ca^{2+}]_{SR}$  approached control levels; i.e., at  $[Ca^{2+}]_{SR}$  in excess of 80% of control levels. As with the STOCs, the amplitude of the  $Ca^{2+}$  sparks recovered as the stores reloaded, as expected for an increase in the electrochemical driving force on  $Ca^{2+}$  across the SR membrane.

## DISCUSSION

### *Ca<sup>2+</sup> Sparks Trigger STOCs*

When spontaneous miniature outward currents due to BK channel openings were first observed in neurons almost two decades ago, Brown et al. (1983) demon-

strated that the source of the  $Ca^{2+}$  was intracellular and speculated that “packets of  $Ca^{2+}$ ” were released from intracellular stores and acted as intracellular messengers. When STOCs were first reported in smooth muscle cells over a decade ago (Benham and Bolton, 1986), a similar explanation was advanced. The observation of  $Ca^{2+}$  “puffs” in *Xenopus* oocytes (Parker and Yao, 1991) and  $Ca^{2+}$  sparks in cardiac (Cheng et al., 1993) and skeletal (Tsugorka et al., 1995) myocytes was soon followed by the observation of similar  $Ca^{2+}$  sparks in single smooth muscle cells by Nelson et al. (1995), and then by Mirroneau et al. (1996). In the present study, we used a high-speed imaging system to record  $Ca^{2+}$  sparks and STOCs simultaneously in the same cell, which allowed us to compare them in detail. We found that there is a close association between the oc-

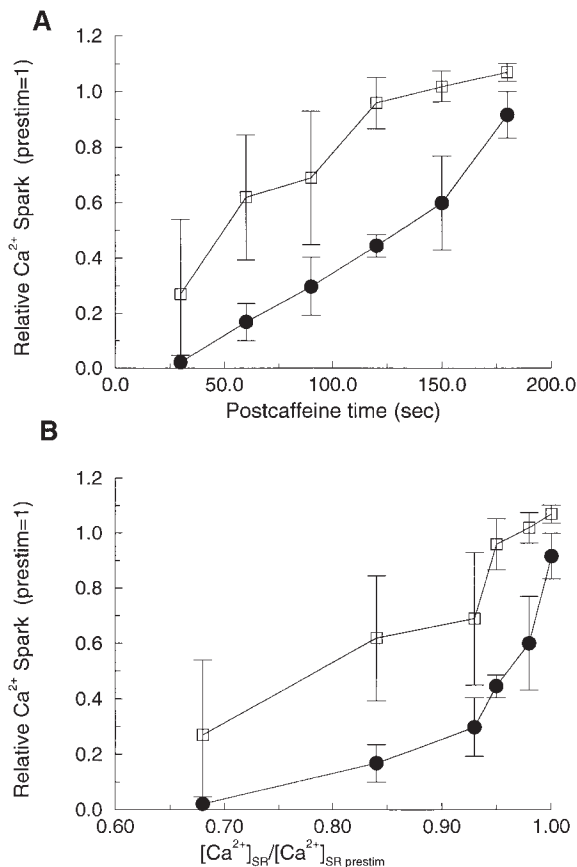


FIGURE 8. Relationship between  $[Ca^{2+}]_{SR}$  and  $Ca^{2+}$  sparks. (A) Relationship between time after a 3-s caffeine application and amplitude ( $\square$ ) and frequency ( $\bullet$ ) for  $Ca^{2+}$  sparks. After the caffeine application,  $Ca^{2+}$  sparks ceased, and then recovered as the SR refilled. (B) Relationship between fractional  $[Ca^{2+}]_{SR}$  and spark frequency ( $\bullet$ ) and amplitude ( $\square$ ) and frequency of  $Ca^{2+}$  sparks were normalized to values before the application of caffeine ( $n = 4$  cells).

currence of  $Ca^{2+}$  sparks and STOCs and that  $Ca^{2+}$  sparks and their corresponding STOCs have similar time courses. (In other smooth muscle types, however, the  $Ca^{2+}$  sparks have a longer time course than the STOCs they cause; Kirber et al., 1998). Furthermore, changes in  $Ca^{2+}$  spark frequency and amplitude were always paralleled by changes in STOC frequency and amplitude when the SR was depleted by caffeine and subsequently refilled. Thus, our findings provide additional evidence for the causal link between  $Ca^{2+}$  sparks and STOCs.

#### How Can a 100-nM Increase Over the Resting Cytosolic $[Ca^{2+}]$ Cause a STOC?

The peak spark amplitude measured with fluo-3 averaged  $\sim 10\%$  ( $\Delta F/F_0 \times 100$ ), and the resting  $[Ca^{2+}]_{CYTO}$  measured ratiometrically with fura-2 in these cells is consistently  $\sim 100$  nM (Drummond and Fay, 1996). Us-

ing this value for resting  $[Ca^{2+}]$ , the mean  $\Delta F/F_0$  converts to a mean change in  $[Ca^{2+}]$ , at the peak, of  $\sim 100$  nM,<sup>2</sup> leading to a mean total  $[Ca^{2+}]$  at the peak of  $\sim 200$  nM in the brightest pixel in a given spark, assuming equilibrium between  $Ca^{2+}$  and fluo-3. Is this sufficient to cause openings of BK channels in this cell type at 0 mV, the potential at which we measured STOCs and  $Ca^{2+}$  sparks simultaneously? The best answer to this question comes from consideration of earlier studies of BK channels in excised, inside-out patches in the same cells used here (Singer and Walsh, 1987). There, the probability of a channel's being in the open state ( $P_o$ ) at 0 mV in the presence of 100 nM  $Ca^{2+}$  was essentially 0 (see Fig. 6 in Singer and Walsh, 1987), and an order of magnitude increase in  $[Ca^{2+}]$  to 1  $\mu$ M caused a  $P_o$  of only  $\sim 0.1$ . Thus, it appears that a  $[Ca^{2+}]_{CYTO}$  of  $\sim 200$  nM is not sufficient to cause substantial BK channel opening at 0 mV.

How are we to explain this apparent contradiction? Three considerations lead strongly to the explanation that the BK channels lie close enough to the SR  $Ca^{2+}$  release site so that the channels sense a much higher concentration than the average we measured. First, there is considerable work on modeling the diffusion-reaction events that occur near a point source of  $Ca^{2+}$  release in the presence of calcium buffering (Stern, 1992; Naraghi and Neher, 1997). The results from such studies indicate that the fluo-3 is not in equilibrium with  $Ca^{2+}$  emerging from the point of SR release at distances smaller than our pixel sizes ( $333 \times 333$  nm). Thus,  $[Ca^{2+}]_{CYTO}$  very close to the point of SR release could be many micromolar, given that  $Ca^{2+}$  currents through the release channels are in the range of 1 pA (Mejia-Alvarez et al., 1998). If the BK channels are very close to an SR release site, then they will sense a  $[Ca^{2+}]$  in the micromolar range that is sufficient to activate them at 0 mV.

<sup>2</sup>The ability of the ultrafast microscope to resolve and measure highly localized calcium signals was examined using a computer simulation of  $Ca^{2+}$  sparks of known peak  $[Ca^{2+}]$  as imaged inside a model cell. Fluorescence ratios ( $\Delta F/F_0$ ) were calculated from simulated images of a range of spark  $[Ca^{2+}]$  amplitudes, both in and out of focus. From these simulations, we estimated that an observed average spark amplitude of 10% ( $\Delta F/F_0$ ) is consistent with a peak spark  $[Ca^{2+}]$  of 200 nM, or 100 nM above resting  $[Ca^{2+}]$ . This estimate was made in the following way.

First, the fluorescence intensity distribution of a typical  $Ca^{2+}$  spark inside a smooth muscle cell was simulated. Custom software was used to calculate the three-dimensional image of a model smooth muscle cell filled with 50  $\mu$ M fluo-3 ( $K_d = 390$  nM) in equilibrium with a resting  $[Ca^{2+}]$  of 100 nM. The cell was modeled as a cylinder with cross-sectional diameters of 10  $\mu$ m in the transverse direction and 6  $\mu$ m in the axial direction, the direction of focus in the microscope, and of infinite length with respect to the imaging. These dimensions were previously derived from three-dimensional reconstructions of toad gastric smooth muscle cells (our unpublished data). The three-dimensional fluorescence intensity distribution was calculated assuming bound fluo-3 was 100 $\times$  as fluorescent as the free species. At resting  $[Ca^{2+}]$ ,

Second, in earlier studies on excised inside-out patches in these cells, we calculated the minimum density of the BK channels to be on the order of 1 channel/ $\mu\text{m}^2$ , based on an assumption of uniform channel density (Singer and Walsh, 1987). But such a uniform distribution would place only three BK channels in the  $3\text{-}\mu\text{m}^2$  region, which is the area over which the  $\text{Ca}^{2+}$  elevation occurs during the spark. Since even at a  $[\text{Ca}^{2+}]_{\text{CYTO}}$  of  $1\ \mu\text{M}$ , the  $P_o$  is 0.1, less than one BK channel would be open at any one time in this region. And in most of this  $3\text{-}\mu\text{m}^2$  region, the increase in  $[\text{Ca}^{2+}]$  is less than that at the center of the spark, where it averages 200 nM. But the mean STOC amplitude is  $\sim 30$  pA, requiring six BK channels to be open simultaneously.

Third, and perhaps most convincingly, is the simple observation that inverted STOCs of substantial amplitude (20–30 pA) can be recorded even at  $-80$  mV (Fig. 3) when the external  $\text{K}^+$  is elevated. At this potential, the  $\text{Ca}^{2+}$  sparks average 10% (Fig. 4). However, from earlier studies on excised patches, we know that  $10\ \mu\text{M}$   $[\text{Ca}^{2+}]_{\text{CYTO}}$  is required for a  $P_o$  of 0.1 at this potential (see Fig. 6 in Singer and Walsh, 1987). Hence, the BK channels must lie close to the SR release site. In summary, these considerations lead to two conclusions: an SR  $\text{Ca}^{2+}$  release site causing a  $\text{Ca}^{2+}$  spark must lie close to BK channels, and the BK channels responsible for a STOC must be clustered. Thus, the spark-STOC site may be a distinct morphological specialization much like a synaptic vesicle release site.

#### *Cytosolic $[\text{Ca}^{2+}]$ Recovers an Order of Magnitude Faster than SR $[\text{Ca}^{2+}]$ after Caffeine-induced SR Depletion*

This study provides the first direct measure of the temporal relationship between  $[\text{Ca}^{2+}]_{\text{CYTO}}$  and  $[\text{Ca}^{2+}]_{\text{SR}}$  in response to depletion of SR  $\text{Ca}^{2+}$  stores in smooth mus-

cle cells and in myocytes of any type. After stimulation with caffeine, recovery of SR  $\text{Ca}^{2+}$  was  $\sim 10\times$  slower than cytosolic  $\text{Ca}^{2+}$ . Thus, the correspondence of  $\text{Ca}^{2+}$  spark and STOC frequency with  $[\text{Ca}^{2+}]_{\text{SR}}$  rather than with  $[\text{Ca}^{2+}]_{\text{CYTO}}$  was readily apparent. Since the rise in  $[\text{Ca}^{2+}]_{\text{CYTO}}$  due to release from the SR fell back to rest well before  $[\text{Ca}^{2+}]_{\text{SR}}$  recovered, much of the cytosolic  $\text{Ca}^{2+}$  must be either bound to myoplasmic buffering sites with slow off rates or cleared into another, optically silent compartment before gradually reappearing as SR  $\text{Ca}^{2+}$ . Some fraction of the  $\text{Ca}^{2+}$  that refills the SR may come directly from the cell exterior, although we detected no macroscopic inward current at a holding potential of  $-80$  mV after caffeine-induced depletion. There is evidence in these cells to indicate that mitochondria constitute the third compartment. It has been demonstrated that mitochondria sequester a portion of the elevated  $\text{Ca}^{2+}$  caused by activation of voltage-gated  $\text{Ca}^{2+}$  channels in these cells (Drummond and Fay, 1996). More recently, it has been shown that mitochondria sequester  $\text{Ca}^{2+}$  released from the SR so that the time course or recovery of SR and mitochondrial  $\text{Ca}^{2+}$  parallel one another as the sequestered  $\text{Ca}^{2+}$  exits the mitochondria and recharges the SR (Drummond et al., 1997). This mechanism is consistent with observations that SR and mitochondria are located in close apposition in smooth muscle cells (Nixon et al., 1994; see also Rizzuto et al., 1998). Given these facts, it is also possible that mitochondria make a contribution to the regulation of  $\text{Ca}^{2+}$  sparks, although there is no evidence for this as yet.

#### *What Is the Link between $[\text{Ca}^{2+}]_{\text{SR}}$ and the Frequency of $\text{Ca}^{2+}$ Sparks and STOCs?*

Studies on RyRs in artificial lipid bilayers support our conclusion that at least a portion of the increase in fre-

---

$\sim 25\%$  of the fluo-3 was bound to  $\text{Ca}^{2+}$  and the fluorescence signal at rest was  $\sim 20\%$  of the maximum attainable with saturating  $\text{Ca}^{2+}$ .

Second, the spatial  $[\text{Ca}^{2+}]$  profile of a  $\text{Ca}^{2+}$  spark was added to the simulated resting cell. A  $\text{Ca}^{2+}$  spark was modeled as a stationary, Gaussian spot of calcium with a known peak  $[\text{Ca}^{2+}]$  and a spatial full width at half-maximum amplitude of  $1.7\ \mu\text{m}$ . This simulates the spark at a single point in time, corresponding to the observed images of sparks at the time of peak fluorescence intensity. The  $\text{Ca}^{2+}$  spark was added to the resting cell model with the spark peak at the center of the cell, and the corresponding three-dimensional image of fluo-3 distribution was calculated as for the resting cell alone. The center of the cell was used to avoid having to simulate the effect of the cell membrane on diffusion. Since the fluorescence background due to resting  $[\text{Ca}^{2+}]$  is likely highest at the center, where the cell is thickest, this is probably the worst case, for our purposes, for measuring  $\Delta\text{F}/\text{F}_0$ .

Next, the image formation and acquisition was simulated. The three-dimensional fluorescence image of the cell and spark was blurred with the three-dimensional image of a theoretical, wide-field, point spread function, for a 1.3 NA objective lens (Nikon Inc.) calculated at 530 nm wavelength (Tella, 1985). The image resolution was decreased to 300-nm pixels, by adding three-by-three groups of pix-

---

els, in order to simulate the image formation (point spread function) and acquisition (camera pixelization) process. The resulting three-dimensional image contained images of the spark in and out of focus, as seen against the fluorescence background arising from the global resting  $[\text{Ca}^{2+}]$ .

Lastly, using the blurred images of the cell with and without the spark, the fluorescence ratios ( $\Delta\text{F}/\text{F}_0$ ) were calculated at the pixel corresponding to the spark center, at 200-nm focus steps through the  $6\text{-}\mu\text{m}$  depth of the cell. The effect of uncertainty in focus was examined by weighting the  $\Delta\text{F}/\text{F}_0$  calculated at each depth through the cell by the probability of a spark occurring at that depth. Although the modeled spark was located in the cell center, the model used for spark spatial distribution assumed that sparks were constrained to occur at the outer edge of the cell, adjacent to the plasma membrane, and were equally likely to occur anywhere along the plasma membrane. A spark with a known peak  $[\text{Ca}^{2+}]$  of 200 nM (100 nM above resting  $[\text{Ca}^{2+}]$ ) yielded a  $\Delta\text{F}/\text{F}_0$  of 18% when in focus (centered in depth) and 5.5% when  $3\ \mu\text{m}$  out of focus (top or bottom of cell). After accounting for the effects of spark location on focus, the average  $\Delta\text{F}/\text{F}_0$  was 10%, a value equivalent to the average observed spark peak amplitude described in this report.

quency of  $\text{Ca}^{2+}$  sparks (and consequently STOCs) that we observe at higher  $[\text{Ca}^{2+}]_{\text{SR}}$  is due to regulation of RyR gating by  $[\text{Ca}^{2+}]_{\text{SR}}$ . RyRs from the cells used in the present study have been partially purified from microsomal membranes and reconstituted into lipid bilayers, where they gave rise to single channel currents whose frequency of opening increased as the  $[\text{Ca}^{2+}]$  was elevated on the side of the bilayer corresponding to the luminal surface (Xu et al., 1994). Moreover, the RyRs from this amphibian preparation appear to be quite like those in mammalian cardiac cells, although not identical to them (Xu et al., 1994). In both cardiac and skeletal muscle, there is a great deal of evidence from studies in artificial bilayers that luminal  $[\text{Ca}^{2+}]$  increases the probability of RyR channels being in the open state, although the precise site of this action remains in doubt (Ikemoto et al., 1991; Gilchrist et al., 1992; Sitsapesan and Williams, 1994; 1995; Donoso et al., 1995; Lukyanenko et al., 1996; Tripathy and Meissner, 1996). Nevertheless, we cannot exclude the possibility that the lower apparent frequency of  $\text{Ca}^{2+}$  sparks at lower SR  $\text{Ca}^{2+}$  levels is due to small amplitude events (resulting from decreased driving force on SR  $\text{Ca}^{2+}$ ) that escape detection (Song et al., 1997). However, if this explanation is true, then the same measurement bias affected two separate and independent measures; that is, electrophysiological recording of STOCs and optical detection of  $\text{Ca}^{2+}$  sparks, in the same way. Finally, the precise mechanism of SR  $\text{Ca}^{2+}$  action might matter little as far as the physiological outcome is concerned. That is, an increase in  $[\text{Ca}^{2+}]_{\text{SR}}$  leads to an increase in total outward current whether due to an increase in STOC frequency or amplitude or both, and

an increase in outward current will lead to hyperpolarization of the membrane with all the attendant consequences (see Nelson et al., 1995).

#### *Physiological Role of $[\text{Ca}^{2+}]_{\text{SR}}$ as a Regulator of $\text{Ca}^{2+}$ Sparks in Smooth Muscle Cells*

The present study makes it clear that as the SR stores attain higher levels of free  $\text{Ca}^{2+}$  there will be an increase in both the frequency and amplitude of  $\text{Ca}^{2+}$  sparks and the STOCs that they cause. Moreover, the relationship between  $[\text{Ca}^{2+}]_{\text{SR}}$  and spark (and STOC) frequency becomes quite steep when the SR refills to 80% or more of its resting level. Thus,  $[\text{Ca}^{2+}]_{\text{SR}}$  is potentially an important regulator of spark (and STOC) frequency. However, this study should not be taken to mean that  $[\text{Ca}^{2+}]_{\text{SR}}$  is the only regulator of sparks and STOCs. This caveat is quite important when considering the role of voltage-activated  $\text{Ca}^{2+}$  channels in regulating sparks. For there is now evidence that  $\text{Ca}^{2+}$  entry through voltage-gated  $\text{Ca}^{2+}$  channels in smooth muscle can elicit  $\text{Ca}^{2+}$  sparks even when the depolarizations used to activate these  $\text{Ca}^{2+}$  channels are quite brief (Arnaudeau et al., 1997; ZhuGe et al., 1998b). This sort of spark induction by depolarization would appear to be due to a local control mechanism, perhaps together with increased SR  $\text{Ca}^{2+}$  load, as is the case in cardiac cells (see Cannell et al., 1995). In other instances, however, it may be that global  $[\text{Ca}^{2+}]_{\text{SR}}$  is the dominant intermediary in regulation of spark frequency. For example, it is possible, although as yet unproven, that some neurotransmitters or cyclic nucleotides, which alter spark frequency (Porter et al., 1998), act in part by altering  $[\text{Ca}^{2+}]_{\text{SR}}$ .

---

We thank Jeffrey Carmichael, Rebecca McKinney, Brian Packard, Paul Tilander, and Yu Yan for excellent technical assistance. We thank Michael Kirber, Robert Drummond, Stephen Sims, and Lawrence Lifshitz for helpful comments and discussion. We dedicate this paper to our colleague, Fredric S. Fay, who died tragically midway through this study and whose friendship, vision, and passion for science made him an ideal colleague.

This study was supported in part by National Institutes of Health grants to F.S. Fay and J.V. Walsh, Jr., and a National Science Foundation grant to R.A. Tuft and Walter Carrington.

*Original version received 2 July 1998 and accepted version received 12 November 1998.*

#### REFERENCES

- Arnaudeau, S., F.X. Boittin, N. Macrez, J.L. Lavie, C. Mironneau, and J. Mironneau. 1997. L-type and  $\text{Ca}^{2+}$  release channel-dependent hierarchical  $\text{Ca}^{2+}$  signaling in rat portal vein myocytes. *Cell Calc.* 22:399–411.
- Becker, P.L., and F.S. Fay. 1987. Photobleaching of Fura-2 and its effect on determination of calcium concentrations. *Am. J. Physiol.* 253:C613–C618.
- Becker, P.L., J.V. Walsh, J.J. Singer, and F.S. Fay. 1989. Regulation of  $[\text{Ca}^{2+}]$  in voltage-clamped single smooth muscle cells. *Science.* 244:211–214.
- Benham, C.D., and T.B. Bolton. 1986. Spontaneous transient outward currents in single visceral and vascular smooth muscle cells of rabbit. *J. Physiol. (Camb.)* 381:385–406.
- Berridge, M.J. 1997. Elementary and global aspects of calcium signaling. *J. Physiol. (Camb.)* 499:291–306.
- Bolton, T.B., and Y. Imaizumi. 1996. Spontaneous transient outward currents in smooth muscle cells. *Cell Calc.* 20:141–152.
- Brown, D.A., A. Constanti, and P.R. Adams. 1983. Ca-activated potassium current in vertebrate sympathetic neurones. *Cell Calc.* 4:407–420.
- Cannell, M.B., H. Cheng, and W.J. Lederer. 1995. The control of calcium release in heart muscle. *Science.* 268:1045–1049.
- Chatton, J.-Y., H. Liu, and J.W. Stucki. 1995. Simultaneous measurements of  $\text{Ca}^{2+}$  in the intracellular stores and the cytosol of

- hepatocytes during hormone-induced  $\text{Ca}^{2+}$  oscillations. *FEBS Lett.* 368:165–168.
- Cheng, H., W.J. Lederer, and M.B. Cannell. 1993. Calcium sparks: elementary events underlying excitation–contraction coupling in heart muscle. *Science.* 262:740–744.
- Cheng, H., M.R. Lederer, W.J. Lederer, and M.B. Cannell. 1996. Calcium sparks and  $[\text{Ca}^{2+}]_i$  waves in cardiac myocytes. *Am. J. Physiol.* 270:C148–C159.
- Donoso, P., H. Prieto, and C. Hidalgo. 1995. Luminal calcium regulates calcium release in triads isolated from frog and rabbit skeletal muscle. *Biophys. J.* 68:507–515.
- Drummond, R.M., and F.S. Fay. 1996. Mitochondria contribute to  $\text{Ca}^{2+}$  removal in smooth muscle cells. *Pflügers Arch.* 431:473–482.
- Drummond, R.M., D.S. Bowman, R.A. Tuft, and F.S. Fay. 1997. Relationship of mitochondrial  $\text{Ca}^{2+}$  homeostasis to  $[\text{Ca}^{2+}]_i$  in the cytosol and sarcoplasmic reticulum in smooth muscle cells. *Biophys. J.* 72:185. (Abstr.)
- Fay, F.S., R. Hoffman, S. Leclair, and P. Merriam. 1982. Preparation of individual smooth muscle cells from the stomach of *Bufo marinus*. *Methods Enzymol.* 85:284–291.
- Galvez, A., G. Gimenez-Gallego, J.P. Reuben, L. Roy-Contancin, P. Feigenbaum, G.J. Kaczorowski, and M.L. Garcia. 1990. Purification and characterization of a unique, potent, peptidyl probe for the high conductance calcium-activated potassium channel from venom of the scorpion *Buthus tamulus*. *J. Biol. Chem.* 265:11083–11090.
- Gilchrist, J.S.C., A.N. Belcastro, and S. Katz. 1992. Intraluminal  $\text{Ca}^{2+}$  dependence of  $\text{Ca}^{2+}$  and ryanodine-mediated regulation of skeletal muscle sarcoplasmic reticulum  $\text{Ca}^{2+}$  release. *J. Biol. Chem.* 267:20850–20856.
- Golovina, V.A., and M.P. Blaustein. 1997. Spatially and functionally distinct  $\text{Ca}^{2+}$  stores in sarcoplasmic and endoplasmic reticulum. *Science.* 275:1643–1648.
- Gordienko, D.V., T.B. Bolton, and M.B. Cannell. 1998. Variability in spontaneous subcellular calcium release in guinea-pig ileum smooth muscle cells. *J. Physiol. (Camb.)* 507:707–720.
- Gryniewicz, G., M. Poenie, and R.Y. Tsien. 1985. A new generation of  $\text{Ca}^{2+}$  indicators with greatly improved fluorescence properties. *J. Biol. Chem.* 260:3440–3450.
- Hamill, O.P., A. Marty, E. Neher, B. Sakmann, and F.J. Sigworth. 1981. Improved patch-clamp techniques for high-resolution current recording from cells and cell-free membrane patches. *Pflügers Arch.* 391:85–100.
- Hernandez-Cruz, A., F. Sala, and P.R. Adams. 1990. Subcellular calcium transients visualized by confocal microscopy in a voltage-clamped vertebrate neuron. *Science.* 247:858–862.
- Hofer, A.M., and T.E. Machen. 1993. Technique for in situ measurement of calcium in intracellular inositol 1,4,5-trisphosphate-sensitive stores using the fluorescent indicator mag-fura-2. *Proc. Natl. Acad. Sci. USA.* 90:2598–2602.
- Hofer, A.M., and I. Schulz. 1996. Quantification of intraluminal free  $[\text{Ca}]$  in the agonist-sensitive internal calcium store using compartmentalized fluorescent indicators: some considerations. *Cell Calc.* 20:235–242.
- Ikemoto, N., B. Antoniu, J.-J. Kang, L.G. Meszaros, and M. Ronjat. 1991. Intravesicular calcium transient during calcium release from sarcoplasmic reticulum. *Biochemistry.* 30:5230–5237.
- Kirber, M.T., E.F. Etter, J.J. Singer, F.S. Fay, and J.V. Walsh, Jr. 1996. Sparks and STOCs in esophageal smooth muscle cells. *Dig. Dis. Sci.* 41:1893. (Abstr.)
- Kirber, M.T., K.D. Bellve, L.M. Lifshitz, R.A. Tuft, J.V. Walsh, Jr., and K.E. Fogarty. 1998. High speed 3-D imaging reveals differences between sparks that generate STOCs and those that do not. *Biophys. J.* 74:272. (Abstr.)
- Lukyanenko, V., I. Gyorke, and S. Gyorke. 1996. Regulation of calcium release by calcium inside the sarcoplasmic reticulum in ventricular myocytes. *Pflügers Arch.* 432:1047–1054.
- Mejia-Alvarez, R., C. Kettlun, E. Ríos, M. Stern, and M. Fill. 1998. Unitary calcium currents through cardiac ryanodine receptors under physiological conditions. *Biophys. J.* 74:58. (Abstr.)
- Mironneau, J., S. Arnaudeau, N. Macrez-Lepretre, and F.X. Boittin. 1996.  $\text{Ca}^{2+}$  sparks and  $\text{Ca}^{2+}$  waves activate different  $\text{Ca}^{2+}$ -dependent ion channels in single myocytes from rat portal vein. *Cell Calc.* 20:153–160.
- Mlinar, B., and F.S. Fay. 1995. Recording of free calcium and magnesium in intracellular stores in patch clamped smooth muscle cells. *Biophys. J.* 68:113. (Abstr.)
- Naraghi, M., and E. Neher. 1997. Linearized buffered  $\text{Ca}^{2+}$  diffusion in microdomains and its implications for calculation of  $[\text{Ca}^{2+}]_i$  at the mouth of a calcium channel. *J. Neurosci.* 17:6961–6973.
- Nelson, M.T., H. Cheng, M. Rubart, L.F. Santana, A.D. Bonev, H.J. Knot, and W.J. Lederer. 1995. Relaxation of arterial smooth muscle by calcium sparks. *Science.* 270:633–637.
- Nixon, G.F., G.A. Mignery, and A.V. Somlyo. 1994. Immunogold localization of inositol 1,4,5-trisphosphate receptors and characterization of ultrastructural features of the sarcoplasmic reticulum in phasic and tonic smooth muscle. *J. Muscle Res. Cell Motil.* 15:682–700.
- Parker, I., and Y. Yao. 1991. Regenerative release of calcium from functionally discrete subcellular stores by inositol trisphosphate. *Proc. R. Soc. Lond. B Biol. Sci.* 246:269–274.
- Porter, V.A., A.D. Bonev, H.J. Knot, T.J. Heppner, A.S. Stevenson, T. Kleppisch, W.J. Lederer, and M.T. Nelson. 1998. Frequency modulation of  $\text{Ca}^{2+}$  sparks is involved in regulation of arterial diameter by cyclic nucleotides. *Am. J. Physiol.* 274:C1346–C1355.
- Quamme, G., L.-J. Dai, and S.W. Rabkin. 1993. Dynamics of intracellular free  $\text{Mg}^{2+}$  changes in a vascular smooth muscle cell line. *Am. J. Physiol.* 265:H281–H288.
- Rizzuto, R., P. Pinton, W. Carrington, F.S. Fay, K.E. Fogarty, L.M. Lifshitz, R.A. Tuft, and T. Pozzan. 1998. Close contacts with the endoplasmic reticulum as determinants of mitochondrial  $\text{Ca}^{2+}$  responses. *Science.* 280:1763–1766.
- Santana, L.F., E.G. Kranias, and W.J. Lederer. 1997. Calcium sparks and excitation–contraction coupling in phospholamban-deficient mouse ventricular myocytes. *J. Physiol. (Camb.)* 503:21–29.
- Singer, J.J., and J.V. Walsh, Jr. 1987. Characterization of calcium-activated potassium channels in single smooth muscle cells using the patch-clamp technique. *Pflügers Arch.* 408:98–111.
- Sitsapesan, R., and A.J. Williams. 1994. Regulation of the gating of the sheep cardiac sarcoplasmic reticulum  $\text{Ca}^{2+}$ -release channel by luminal  $\text{Ca}^{2+}$ . *J. Membr. Biol.* 137:215–226.
- Sitsapesan, R., and A.J. Williams. 1995. The gating of the sheep skeletal sarcoplasmic reticulum  $\text{Ca}^{2+}$ -release channel is regulated by luminal  $\text{Ca}^{2+}$ . *J. Membr. Biol.* 146:133–144.
- Song, L.-S., M.D. Stern, E.D. Lakatta, and H. Cheng. 1997. Partial depletion of sarcoplasmic reticulum calcium does not prevent calcium sparks in rat ventricular myocytes. *J. Physiol. (Camb.)* 505:665–675.
- Steenbergen, J.M., and F.S. Fay. 1996. The quantal nature of calcium release to caffeine in single smooth muscle cells results from activation of the sarcoplasmic reticulum  $\text{Ca}^{2+}$ -ATPase. *J. Biol. Chem.* 271:1821–1824.
- Stern, M.D. 1992. Buffering of calcium in the vicinity of a channel pore. *Cell Calc.* 13:183–192.
- Sugiyama, T., and W.F. Goldman. 1995. Measurement of SR free  $\text{Ca}^{2+}$  and  $\text{Mg}^{2+}$  in permeabilized smooth muscle cells with use of fura-2. *Am. J. Physiol.* 269:C698–C705.
- Tella, L.L. 1985. The determination of a microscope's three-dimensional transfer function for use in image restoration. Mas-

- ter's Thesis, Worcester Polytechnic Institute, Worcester, MA.
- Thastrup, O., P.C. Cullen, B.K. Drobak, M.R. Hanley, and A.P. Dawson. 1990. Thapsigargin, a tumor promoter, discharges intracellular  $\text{Ca}^{2+}$  stores by specific inhibition of the endoplasmic reticulum  $\text{Ca}^{2+}$ -ATPase. *Proc. Natl. Acad. Sci. USA.* 87:2466–2470.
- Tripathy, A., and G. Meissner. 1996. Sarcoplasmic reticulum luminal  $\text{Ca}^{2+}$  has access to cytosolic activation and inactivation sites of skeletal muscle  $\text{Ca}^{2+}$  release channel. *Biophys. J.* 70:2600–2615.
- Tsugorka, A., E. Ríos, and L.A. Blatter. 1995. Imaging elementary events of calcium release in skeletal muscle cells. *Science.* 269:1723–1726.
- Williams, D.A., K.E. Fogarty, R.Y. Tsien, and F.S. Fay. 1985. Calcium gradients in single smooth-muscle cells revealed by the digital imaging microscope using fura-2. *Nature.* 318:558–561.
- Xu, L., F.A. Lai, A. Cohn, E. Etter, A. Guerrero, F.S. Fay, and G. Meissner. 1994. Evidence for a  $\text{Ca}^{2+}$ -gated ryanodine-sensitive  $\text{Ca}^{2+}$  release channel in visceral smooth muscle. *Proc. Natl. Acad. Sci. USA.* 91:3294–3298.
- ZhuGe, R., R.A. Tuft, K.E. Fogarty, and J.V. Walsh, Jr. 1998a. Microdomains mediating generation of  $\text{Ca}^{2+}$  sparks and STOCs in smooth muscle cells. *Biophys. J.* 74:272. (Abstr.)
- ZhuGe, R., R.A. Tuft, K.E. Fogarty, and J.V. Walsh, Jr. 1998b. Coupling of voltage-activated  $\text{Ca}^{2+}$  channels with  $\text{Ca}^{2+}$  sparks and  $\text{Ca}^{2+}$  transients in smooth muscle. *J. Gen. Physiol.* 112:13a. (Abstr.)